Modelling of size distribution of blocky retained austenite in Si-containing bainitic steels

L. Guo[a,*], H. Roelofs[b], M. I. Lembke[c], H. K. D. H. Bhadeshia[a]

[a]*Department of Materials Science and Metallurgy, University of Cambridge, 27 Charles Babbage Road, Cambridge CB3 0FS, U.K.*
[b]*R& D, Swiss Steel AG, Emmenweidstr. 90, CH-6020 Emmenbrücke, Switzerland*
[c]*Steeltec AG, Emmenweidstr. 72, CH-6020 Emmenbrücke, Switzerland*

Abstract

A model for estimating the blocky retained austenite size distribution in Si-containing steels has been developed for the first time, based on the geometric partitioning of prior austenite grains by bainite sheaves. A random volume allocation method for the two new compartments formed by the formation of one bainite sheaf is adopted for reasons detailed in the text. Random selection of the compartment for subdivision is also employed at each step. The model has been verified experimentally using Si-containing bainitic steels.

Keywords: Blocky retained austenite, Size distribution, Bainite, Si-containing steel

1. Introduction

Modern high performance steels, based on bainitic or martensitic microstructures, including the carbide-free low-temperature bainitic steels [1, 2], transformation induced plasticity (TRIP) assisted steels [3] and the quenching and partitioning (Q & P) steels [4], usually contain a fraction of retained austenite [1, 2, 3, 4, 5, 6]. Untransformed austenite is retained to room temperature by adding a cementite inhibitor, typically 1.5 wt% of Si or Al, and

---

*Corresponding author
  Email address: `lg446@cam.ac.uk,lei-guo@outlook.com` (L. Guo)

those solutes that increase hardenability also have a role in this respect [7]. The presence of retained austenite in these steels improves their ductility by enhancing the work hardening capacity through the TRIP effect, but the newly formed martensite in its coarse form can be prone to cracking, thereby undermining the toughness of these steels. Retained austenite in these steels can be categorised into blocks between differently oriented bainite sheaves, and thin films between individual bainitic ferrite platelets. The former is unstable compared with the latter due to its larger size and lower carbon content [8]. Chatterjee and Bhadeshia pointed out that the absolute size of the freshly formed martensite dominates the cracking behaviour of these alloys [9]. Since the film retained austenite is small and stable, it is not problematic, but large blocks of austenite are unstable, so it is important to control their sizes to achieve better mechanical properties [10, 11]. Despite the technical importance, there is little modelling work on the estimation of the retained austenite size distribution and its evolution during the course of transformation. The present study is the first attempt to model the size distribution of blocky retained austenite in these steels.

2. Experimental details

Two Si-containing steels (Table 1) were used to produce the bainitic microstructure. Cylindrical samples ($\phi 10 \times 8$ mm) were heat-treated in a ThermecMastor-Z thermal mechanical simulator under a vacuum of about 10^{-3} Pa, with the dilatation recorded by a laser precision measuring device. Samples of steel A were heated to $1000\,°C$ at a rate of $5\,°C\ s^{-1}$, held at this temperature for 10 min, then cooled to $250\,°C$ at a rate of $10\,°C\ s^{-1}$, soaked at the temperature for 48 h before cooling to ambient temperature. Samples of steel B were

heated up to $950\,°C$ at a rate of $5\,°C\ s^{-1}$, held there for $10\,min$, then cooled to $400\,°C$ or $430\,°C$ at a rate of $10\,°C\ s^{-1}$, for $1\,h$ of isothermal transformation, before cooling to ambient temperature. A flat polished facet with a width of $5\,mm$ was made on the side of each sample, so that thermal grooves formed along the austenite grain boundaries can be observed, for the purpose of grain size measurement. The prior austenite grain size ($\bar{L}_{\gamma0}$) was measured using the mean linear intercept method. Samples for metallography were cut at mid-point where the thermocouple was welded on. The retained austenite size distributions for steel A was measured using optical micrographs, while secondary electron micrographs were used for the finer structure of steel B. The volume fraction of bainite was estimated from dilatometric data as described in [12], a procedure which is implemented in the freely available program MAP_STEEL_DILAT [13].

Table 1: Chemical composition of steels (wt%)

	C	Si	Mn	Ni	Mo	Cr	Cu	S	Fe
A	0.8	1.51	2.03	1.05	0.377	0.22	0.03	-	balance
B	0.22	0.97	1.53	0.18	0.14	1.54	0.17	0.15	balance

3. The model

The blocky retained austenite in bainitic microstructure is the residue of the sub-division of austenite grains by the bainite sheaves, similar to the partitioning caused by martensite plates. Fisher *et al.* first developed a geometric partitioning model for the kinetics of martensite transformation [14], which assumes that every martensite plate takes a fraction, m, of the austenite compartment where it forms, and the new compartments formed are equal in size, so that an analytical solution was obtained. But the assumption that all the compartments

3

are the same in size is clearly over simplified, and will lead to very fine blocks, which cannot explain experimentally observed large blocks. Nevertheless, the model only gives an average compartment size, which is insufficient in estimating the block size distribution.

Adopting this geometric partitioning idea, it is reasonable to assume that each new sheaf of bainite will separate the compartment where it forms. The starting volume fraction of the austenite grain is set to unit 1, because a fraction of m will be transformed to bainite, the total volume of the two subregions remaining after bainite sheaf formation, will be $(1 - m)$. As shown in Fig. 1, if one subregion takes a fraction $a(1 - m)$ of the original compartment, the other will have $(1 - a)(1 - m)$, where $0 < a < 1$ is a random number generated by an FORTRAN intrinsic function. The number of compartments and their sizes were tracked in a computer program written for the work. The next compartment to be transformed was selected randomly by generating a random number b $(0 < b < 1)$, which is then scaled up by the total number of compartments N, if $i \leq bN < i+1$, then the ith compartment is selected for the next subdivision. Its volume fraction V_i will be divided into two compartments of volume fractions $a(1 - m)V_i$ and $(1 - a)(1 - m)V_i$, and the total number of compartments N will be increased by 1. At a given bainite volume fraction, the calculated compartment size distribution represents the untransformed austenite size distribution. So given the prior austenite grain size and volume fraction of bainite or martensite, the model can predict blocky retained austenite size distribution. The size of the largest compartment at each step was recorded as well, as that should be the most detrimental.

To compare the size distribution with experimental data, which is usually a one dimensional grain size, linear intercept of each compartment need to be calculated from its volume.

In order to calculate that, each compartment is approximated by a truncated octahedron of the same volume, whose $\bar{L}$ is related to volume V by [15]

$$\bar{L} = (0.4266V)^{1/3} \tag{1}$$
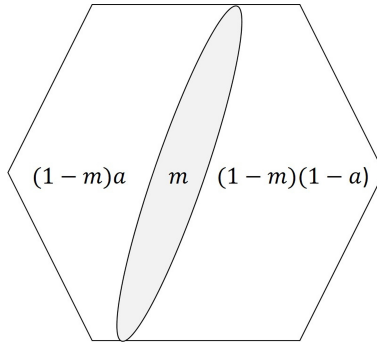
Figure 1: Schematic illustration of random subdivision

3.1. Effect of fraction factor m

The fraction factor m should have a big effect on the model. Fig 2 (a) shows the effect of m on the evolution of the maximum block size as a function of bainite volume fraction. These curves have some plateaus which originates from the intermittent nature of bainite sheaf formation. In the first division, one sheaf can transform a volume fraction m of the austenite, and with the progress of transformation, the average compartment size becomes smaller, Fig. 2 (b). Therefore, a sheaf forms in a small compartment then transforms a smaller volume fraction of the total austenite grain. As the transformation progresses, the total number of compartments increases rapidly, because the compartment to be transformed is selected randomly, the chance for the biggest compartment to be selected becomes even smaller. So in most cases, the largest compartment is not selected for subdivision, giving rise to the

observed plateaus. Smaller m gives larger maximum block size in terms of subdivision steps, but not necessarily in terms of bainite volume fraction. For a smaller m, each subdivision step transforms a smaller volume fraction to bainite, which should gives larger blocks compared to large m, but to obtain the same volume fraction of bainite requires more subdivision steps, which has a two fold effect, it leads to a decrease in the probability of the maximum block to be selected for each subdivision step, but as the number of subdivision needed for the same amount of bainite transformation increases, the probability of the maximum block to be chosen is increased. This two fold contradictory effect could explain the observed inconsistent effect of m on the maximum block size evolution over bainite volume fraction. The average block size decreases continuously as the bainite volume fraction increases as shown in Fig 2 (b), and for a given bainite volume fraction, the increased number of subdivision needed for small m should lead to decrease in the average block size, which is shown in Fig 2 (b), as expected.
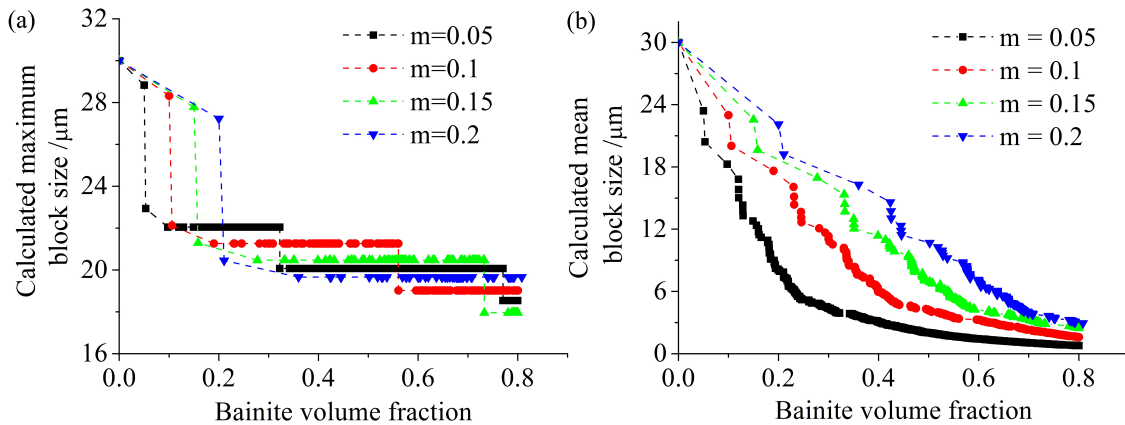
Figure 2: (a) Effect of m on the maximum compartment size. (b) Effect of m on the average block size.

Assume austenite grains can be equivalent to spheres, and the bainite plates are oblate spheroid. The volume of a sphere is $V_s = \frac{4}{3}\pi r^3$, where r is the radius, and that of an oblate spheroid is $V_e = \frac{4}{3}\pi a^2 c$, where a is the semi-axis length, c is the distance from centre to pole

along the symmetry axis. If the bainite plate partitions the austenite grain, then $a = r$, the volume fraction of the oblate spheroid with respect to its circumsphere is $m = \frac{c}{r}$, which is the aspect ratio. The aspect ratio of bainite sheaves was measured from Fig. 5, and corrected by a factor of $\frac{\pi}{2}$ due to stereological effect [16], its mean value was determined to be 0.1.

3.2. General model prediction

The following results were calculated with $m = 0.1$, which means each bainite sheaf transforms a fraction of 0.1 of the compartment in which it forms. Fig. 3 shows the maximum block size evolution for two prior austenite grain sizes ($\bar{L}_{\gamma 0}$) of 50 and 30 μm, the maximum block size decreases as transformation progresses, but it also highly depends on the prior austenite grain size, reducing the prior austenite grain size can refine the retained austenite effectively. The untransformed austenite size distributions for $\bar{L}_{\gamma 0} = 30$ μm for bainite volume fractions of 0.4, 0.6 and 0.8 are shown in Fig. 4 (b), (c) and (d) respectively. As expected, all the size distributions show the number of compartments in a given size of bin decreases as the compartment size increases. The austenite compartment size decreases as bainite volume fraction increases. The maximum austenite compartment sizes for 0.4, 0.6 and 0.8 fraction of bainite transformation are 21, 19 and 19 μm respectively, the number of compartments whose size are larger than 19 μm are 1, 1 and 1 respectively. As the bainite volume fraction V_{α_b} increases, a greater number of divisions is needed to get the same amount of transformation, thus generating much greater number of compartments. Hence the number of small compartments increases rapidly as illustrated in Figs. 4 (b) to (d). Increase the bainite volume fraction can reduce the average retained austenite size, Fig. 4 (a), but not necessarily the size of the biggest block, Fig. 3, which is dependent on the prior austenite grain size and the bai-

nite volume fraction. In actual steels, chemical segregation together with the non-uniformly distributed defects make nucleation of bainite or martensite heterogeneous. All these factors could render some regions more stable than others, thus enhancing the presence of big blocks.
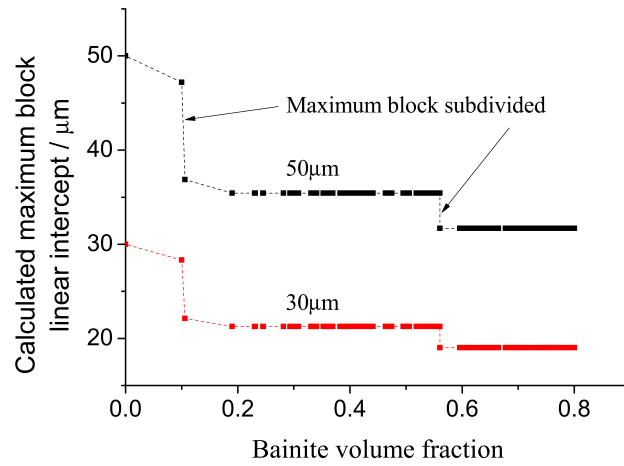
Figure 3: Calculated maximum retained austenite size as a function of bainite volume fraction for $\bar{L}_{\gamma_0} = 50$ and 30 µm.
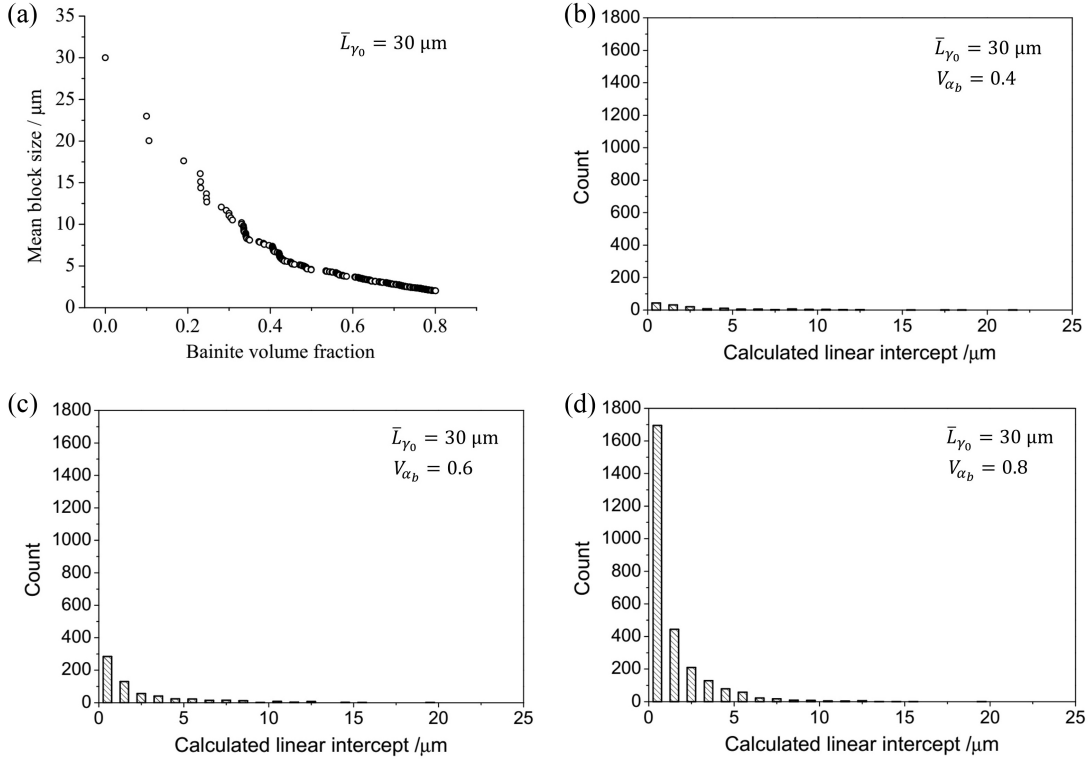
Figure 4: Calculated result for $\bar{L}_{\gamma_0} = 30$ μm. (a) Mean blocky austenite size as a function of bainite volume fraction, (b) Retained austenite size distribution for $V_{\alpha_b} = 0.4$, (c) Retained austenite size distribution for $V_{\alpha_b} = 0.6$, (d) Retained austenite size distribution for $V_{\alpha_b} = 0.8$.

4. Experimental validation

Microstructure from a low temperature carbide-free bainite bainitic steel from Caballero and Bhadeshia is found to have lath bainite [1], which is suitable for validating this geometry partitioning model. The alloy composition is Fe-0.79C-1.59Si-1.94Mn-0.30Mo-1.33Cr-0.11V wt%, the sample was isothermally transformed at 300°C for 14 days, following austenitisation at 1000°C for 15 min. Grain size was estimated to be $50\,$μm from figure 5 (b), because the prior austenite grain size was not reported. Volume fraction of bainite of 0.41 was estimated by the maximum bainite volume given by T_0 line. The size distribution of retained austenite was obtained from Fig. 5 (a) [1]. Because the calculated number of blocks is from

9

a single austenite grain, but the measured blocks are from a section plane of many grains, normalised distributions was used. The measured and calculated size distributions are shown in figure 5 (c) and (d) respectively, note that a minimum size of 0.5 μm was used when doing the image analysis, which was also neglected from the calculated distribution. As can be seen, the general trend of the predicted size distribution matches well with measured one, even though there is some discrepancy in terms of quantitative value. The largest block is correctly predicted, which means in the microstructure, inevitably there will be some big blocky retained austenite. As the biggest blocky austenite is the lest stable one, which should be more detrimental to mechanical property, so it is important to predict it. In this sense, the model could be very useful.
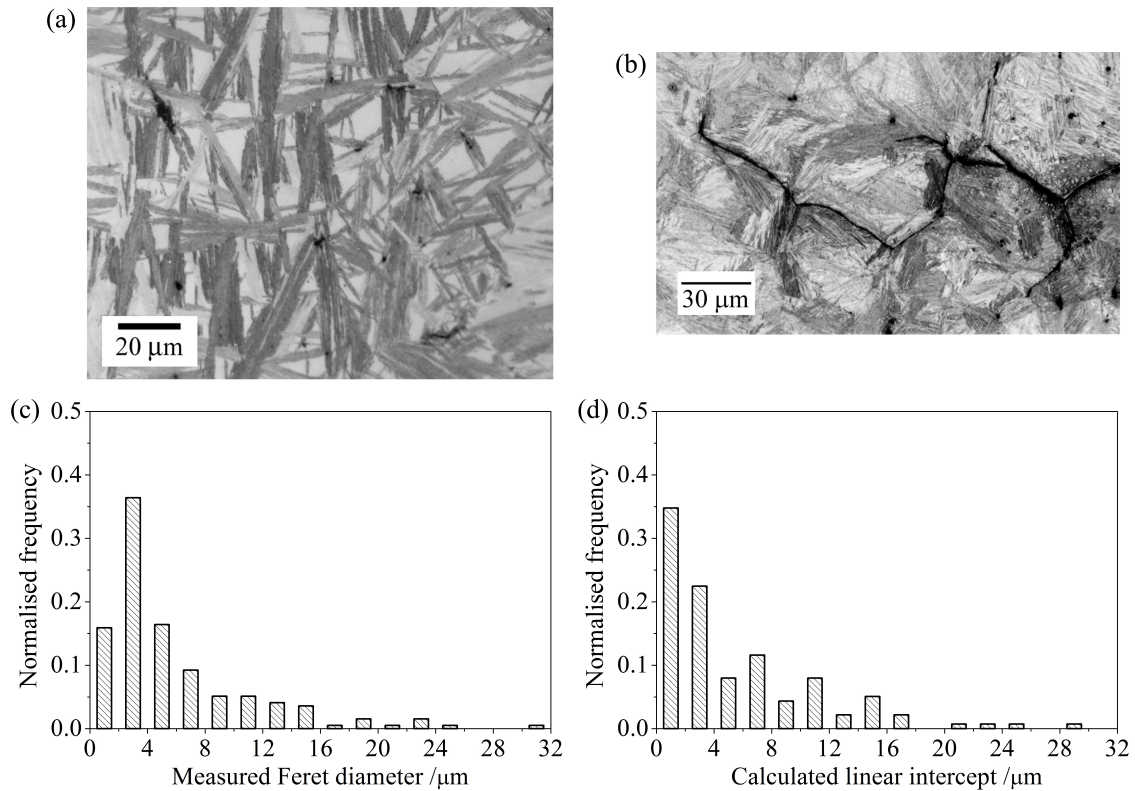
Figure 5: (a) Micrograph from reference used to determine blocky austenite size distribution [1]. Fe-0.79C-1.59Si-1.94Mn-0.30Mo-1.33Cr-0.11V wt% Isothermally transformed at 300°C for 14 days, following austenitisation at 1000°C for 15 min. (b) Micrograph from reference showing austenite grain boundary, which was used to estimate grain size [1]. (c) Measured blocky austenite size distribution. (d) Calculated size distribution, assuming bainite transformation has reached maximum amount given by T_0 line, with $\bar{L}_{\gamma 0} = 40\,\mu$m.

For experimental steels A and B, the prior austenite grain sizes are obtained by the thermal grooving technique, and volume fraction of bainite measured by dilatometry. Prior austenite grain sizes were measured to be $24 \pm 2\,\mu$m for steel A austenitised at $1000\,°$C for $10\,$min, and $12.2 \pm 0.4\,\mu$m for steel B austenitised at $950\,°$C for $10\,$min, Fig. 6 (a) and 6 (c) respectively. The dilatometric strains as a function of time during isothermal treatment at $250\,°$C for steel A is shown in Fig. 6 (b), which when converted gives $V_{\alpha_b} = 0.66$. Similarly, for steel B, Fig. 6 (d) shows the dilatometric strains at $400\,°$C and $430\,°$C, corresponding to V_{α_b} of 0.65 and 0.75.
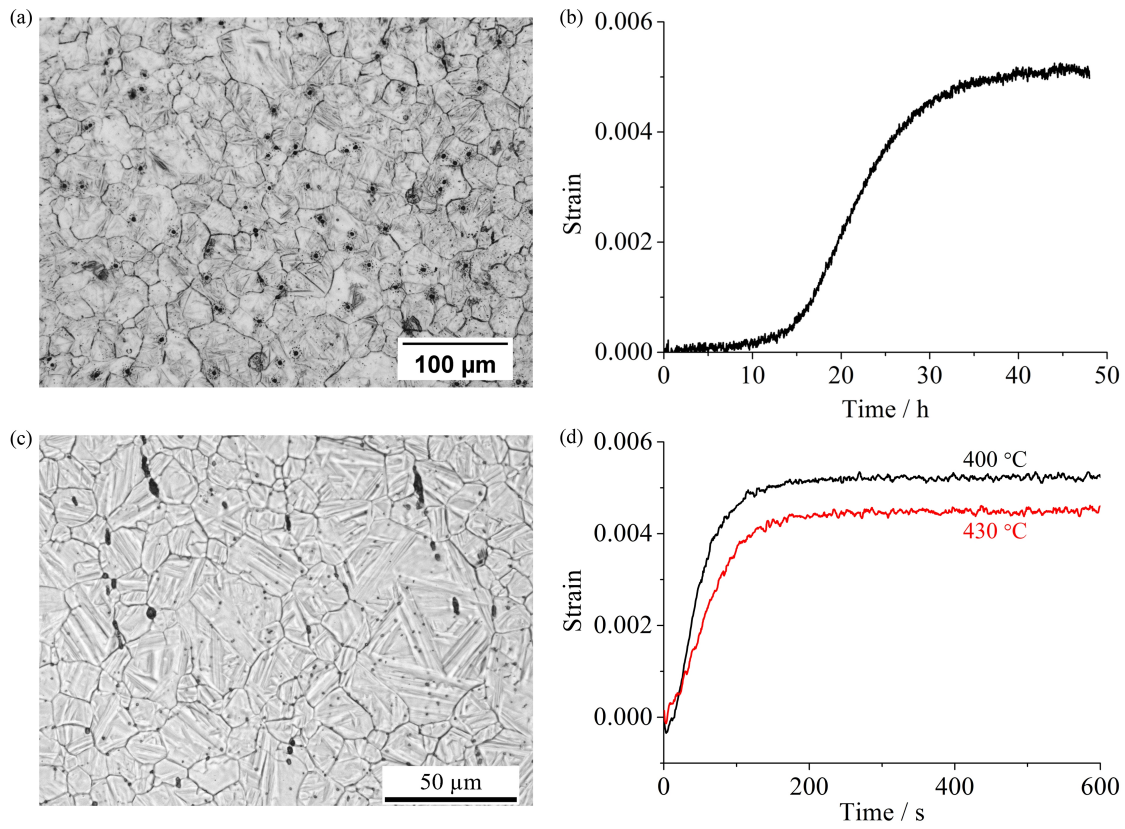
Figure 6: (a) Optical micrograph showing prior austenite grain boundaries of steel A austenitised at 1000 °C for 10 min. (b) Strain as a function of time of steel A isothermally transformed at 250 °C for 48 h. (c) Optical micrograph showing prior austenite grain boundaries of steel B austenitised at 950 °C for 10 min. (d) Strain as a function of time of steel B isothermally transformed at 400 and 430 °C for 1 h.

Steel A has a microstructure consisting of bainite and retained austenite, which can easily be distinguished using optical microscopy, as shown in Fig. 7 (a). The dark areas are bainite and the light ones are retained austenite. The bainite sheaves indeed partition the compartments wherever they form, consistent with the model assumption. A threshold technique was used to select the retained austenite regions, using ImageJ image analysis software[17], the selected area is shown in Fig. 7 (b), and for comparison, Fig. 7 (c) shows a manually drawn image. The measured retained austenite size distribution of steel A by this threshold method is shown in Fig. 8 (a) and that by drawing manually is shown in Fig. 8 (c).

12

The distributions from these two methods are similar, except that the manual method omits the very small particles, so the distribution has low counts at below $1.5\,\mu m$. The measured maximum block sizes for manual and threshold methods are $13.5\,\mu m$ and $14.3\,\mu m$ respectively. The discrepancy is due to the fact that the drawn blocks are naturally not exactly identical to those selected by the threshold method.

The calculated distribution is shown in Fig. 8 (b), the trend is the same with the measured distribution from threshold method, but has much more small blocks than the manual drawn distribution. By removing the calculated blocks whose sizes are below the measured minimum value, the calculated distribution comes closer to the manual drawn distribution, Fig. 8 (d). The comparison between the calculated and measured distributions shows good agreement, and it is reasonable to believe that this model could work well with lenticular martensitic microstructure as the martensite plates grow across the whole compartments where they form, and that is complete partitioning of the compartment, which is exactly what has been assumed in the model, whereas low temperature bainite sheaves in steel A usually cannot grow across the whole compartment.
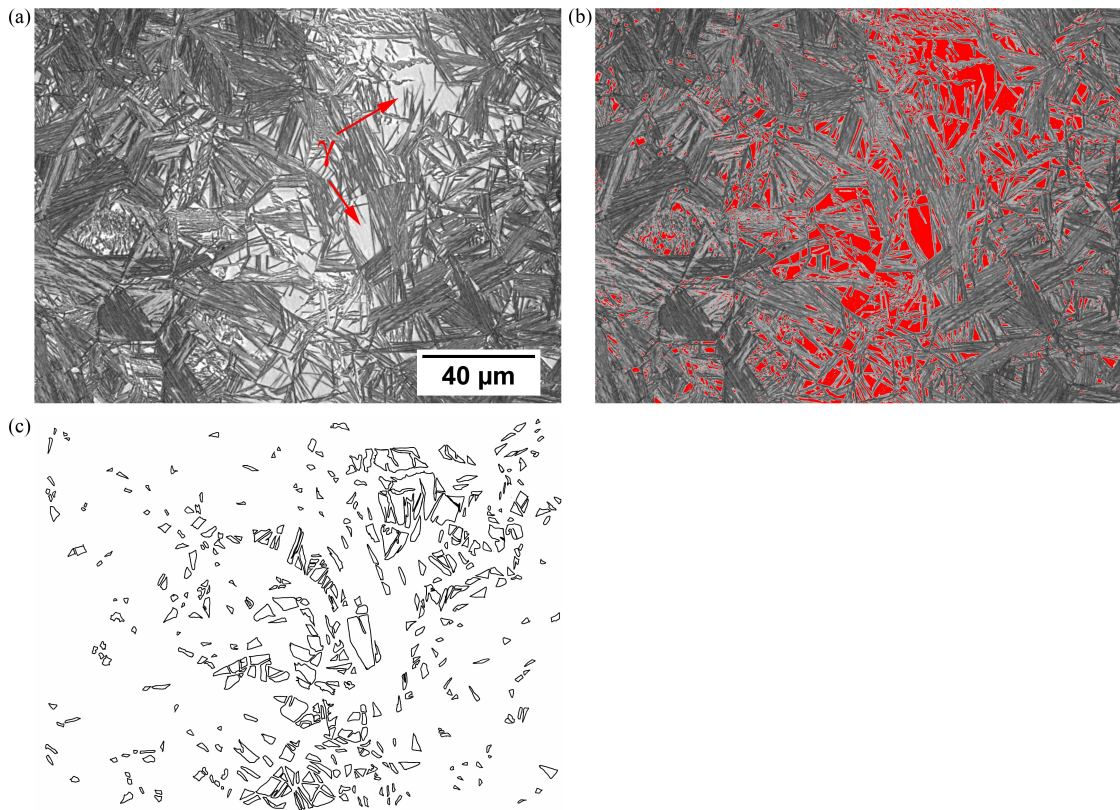
Figure 7: (a) Optical micrograph of steel B transformed at 250 °C for 48 h used for blocky retained austenite size distribution measurement. (b) Selection of blocky retained austenite by ImageJ threshold method. (c) Retained austenite blocks by manual drawing.
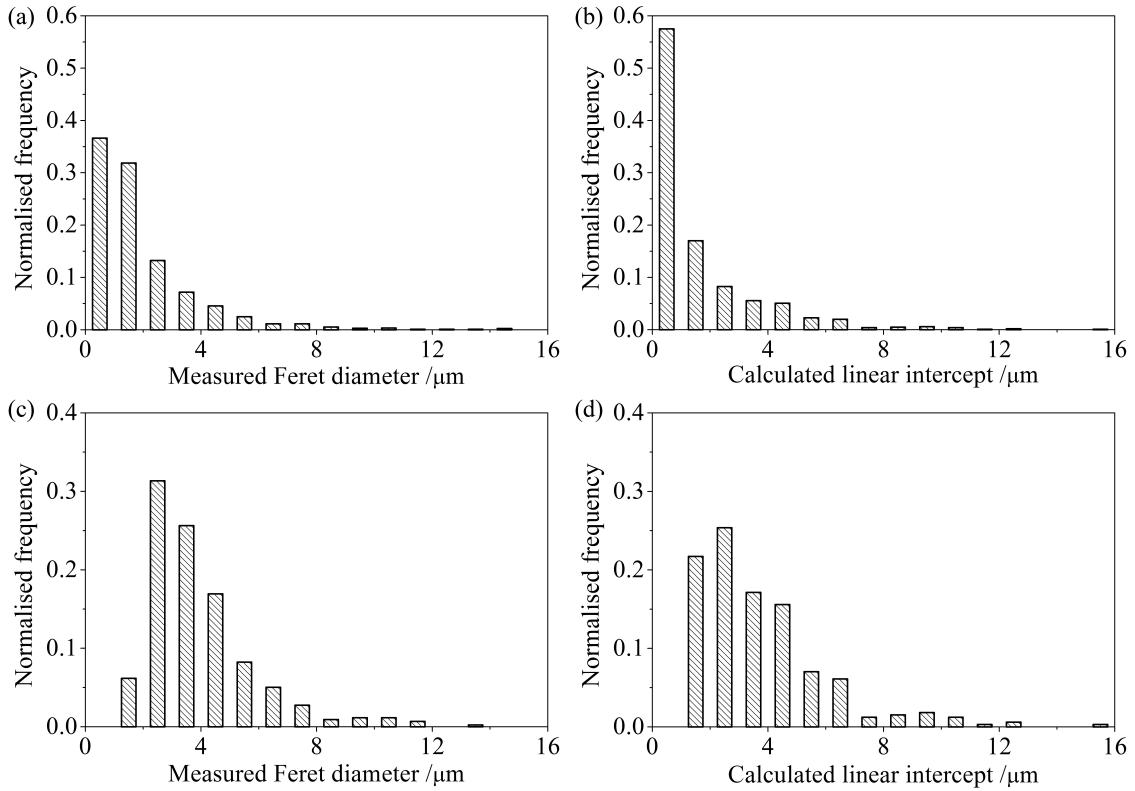
Figure 8: Retained austenite size distribution of steel A isothermally transformed 250 °C for 48 h. (a) Measured using threshold and particle analysis technique in ImageJ software. (b) Calculated with $\bar{L} = 24\,\mu m$ and $V_{\alpha_B} = 0.66$. (c) Measured by manual drawing retained austenite blocks on micrograph. (d) Calculated with compartments smaller than the minimum value of manually measured ones excluded.

The model was also applied to steel B with a different overall morphology of bainite. Fig. 9 (a) and (b) are SEM secondary electron image for steel B transformed at 430 °C and 400 °C respectively. The blocky mixture of $\alpha' + \gamma$ islands were drawn manually as shown in Figs. 9 (c) and 9 (d). The measured size distributions of the blocky mixture of $\alpha' + \gamma$ island for steel B transformed at 430 °C and 400 °C are shown in Fig. 10 (a) and (c) respectively. For transformation at 400 °C, most of the blocks are smaller than 9 μm and the maximum is 11.5 μm, even though the measured $\bar{L}_{\gamma 0}$ is 12.2 μm. For transformation at 430 °C, most of the blocks are below 12 μm, and the maximum size is 18.8, which is much larger than the measured $\bar{L}_{\gamma 0}$. This raises a problem for the model as the measured maximum block size

15

is larger than the average prior austenite grain size, but it also make sense, because prior austenite grain size itself has a distribution, there are grains which are much larger than the mean grain size Fig. 6 (c). Steel A has a homogeneous prior austenite size distribution, and its blocky austenite size distribution was very well predicted by the model, while steel B may have a bimodal prior austenite grain size distribution, hence larger chance of finding grains which are much bigger than the mean size, making it difficult to handle by the model. This signifies the importance to control prior austenite grain size in order to avoid large blocks of retained austenite or $\alpha' + \gamma$ islands.
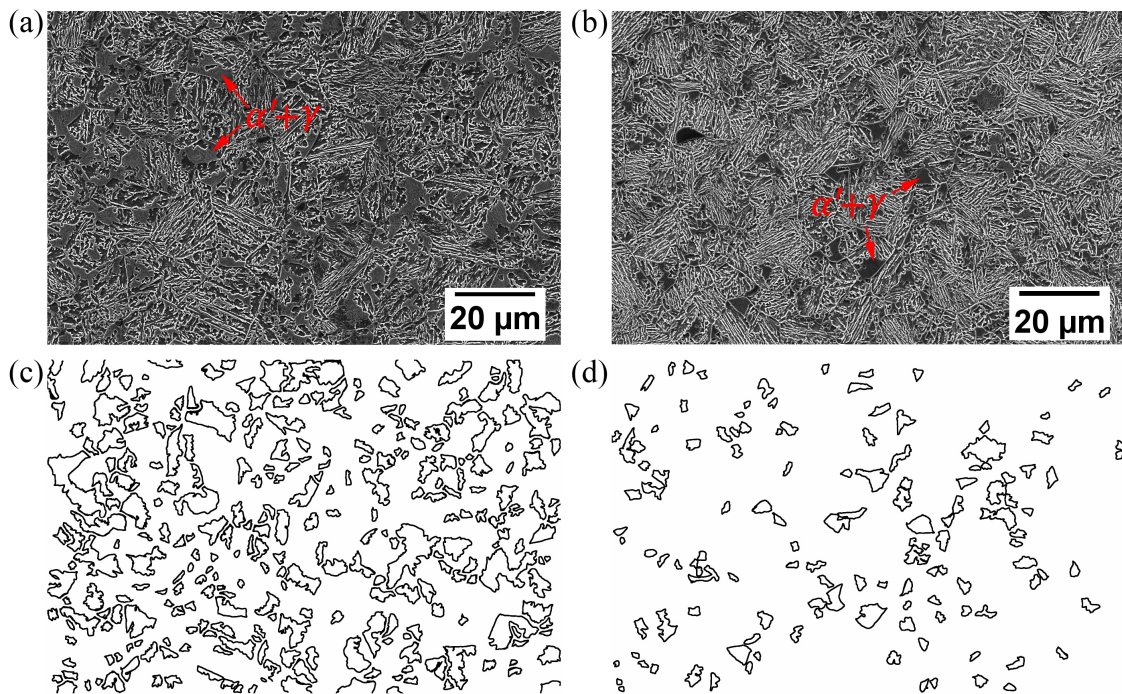
Figure 9: Measurement of $\alpha' + \gamma$ constituent. (a) Secondary electron image of steel B transformed at 430 °C for 1 h, (b) 400 °C for 1 h. (c) $\alpha' + \gamma$ island by manual drawing for (a). (d) $\alpha' + \gamma$ island by manual drawing for (b).
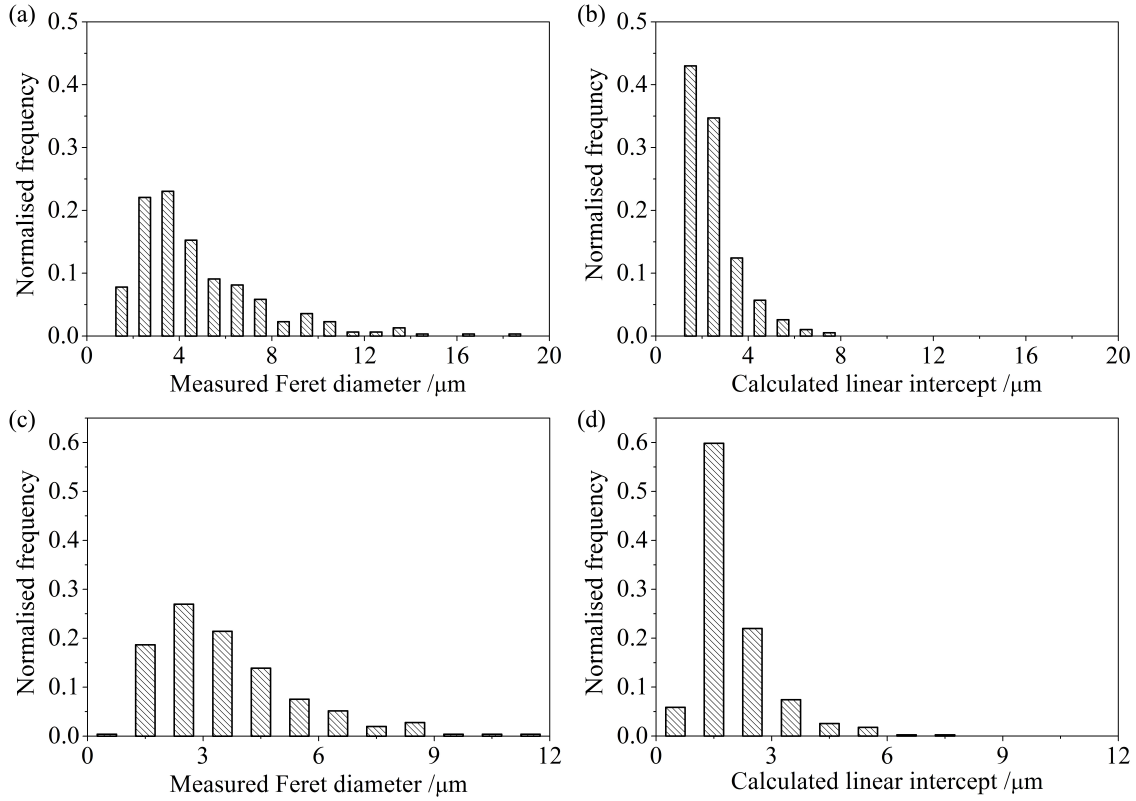
Figure 10: (a) Measured retained austenite size distribution of steel B transformed at 430 °C for 1 h. (b) Calculated retained austenite size distribution with $\bar{L} = 12.2\,\mu\text{m}$ and $V_{\alpha_B} = 0.65$. Compartments which are smaller than the manually measured minimum value are excluded. (c) Measured retained austenite size distribution of steel B transformed at 400 °C for 1 h. (d) Calculated retained austenite size distribution with $\bar{L} = 12.2\,\mu\text{m}$ and $V_{\alpha_B} = 0.75$. Compartments which are smaller than the manually measured minimum value are excluded.

5. Conclusions

A model for predicting blocky austenite size distribution has been developed by a random geometrical subdivision method. Good agreement of the size distributions and the maximum sizes of retained austenite between model predictions and experimental results have been achieved for high carbon lenticular shape of bainite transformed at relatively low temperature. Broad agreement was reached for low carbon lath bainite obtained at relatively high temperature. Predictions from the model emphasis the need to refine prior austenite grain in order to avoid large undesirable retained austenite blocks or $\alpha' + \gamma$ islands.

17

References

[1] F. G. Caballero, H. K. D. H. Bhadeshia, K. J. A. Mawella, D. G. Jones, P. Brown, Very strong low temperature bainite, Materials science and technology 18 (3) (2002) 279–284. URL `http://www.maneyonline.com/doi/abs/10.1179/026708301225000725`

[2] F. Caballero, H. Bhadeshia, Very strong bainite, Current Opinion in Solid State and Materials Science 8 (3) (2004) 251–257.

[3] O. Matsumura, Y. Sakuma, H. Takechi, Trip and its kinetic aspects in austempered 0.4 c-1.5 si-0.8 mn steel, Scripta Metallurgica 21 (10) (1987) 1301–1306.

[4] J. Speer, A. Streicher, D. Matlock, F. Rizzo, G. Krauss, Quenching and partitioning: a fundamentally new process to create high strength trip sheet microstructures., in: Symposium on the Thermodynamics, Kinetics, Characterization and Modeling of: Austenite Formation and Decomposition, 2003, pp. 505–522.

[5] O. Grässel, L. Krüger, G. Frommeyer, L. W. Meyer, High strength Fe–Mn–(Al, Si) TRIP/TWIP steels development - properties - application, International Journal of Plasticity 16 (10) (2000) 1391–1409.

[6] D. Edmonds, K. He, F. Rizzo, B. De Cooman, D. Matlock, J. Speer, Quenching and partitioning martensite- novel steel heat treatment, Materials Science and Engineering: A 438 (2006) 25–34.

[7] E. Girault, A. Mertens, P. Jacques, Y. Houbaert, B. Verlinden, J. V. Humbeeck, Com-

parison of the effects of silicon and aluminium on the tensile behaviour of multiphase TRIP-assisted steels, Scripta materialia 44 (6) (2001) 885–892.

[8] H. Bhadeshia, Nanostructured bainite, in: Proceedings of the Royal Society of London A: Mathematical, Physical and Engineering Sciences, Vol. 466, The Royal Society, 2010, pp. 3–18.

[9] S. Chatterjee, H. K. D. H. Bhadeshia, TRIP-assisted steels: cracking of high-carbon martensite, Materials science and technology 22 (6) (2006) 645–649.

[10] H. K. D. H. Bhadeshia, D. V. Edmonds, Bainite in silicon steels: new composition–property approach part 1, Metal Science 17 (9) (1983) 411–419.
URL http://www.maneyonline.com/doi/abs/10.1179/030634583790420600

[11] H. K. D. H. Bhadeshia, D. V. Edmonds, Bainite in silicon steels: new composition–property approach part 2, Metal Science 17 (9) (1983) 420–425.
URL http://www.maneyonline.com/doi/abs/10.1179/030634583790420646

[12] H. Bhadeshia, S. David, J. Vitek, R. Reed, Stress induced transformation to bainite in Fe–Cr–Mo–C pressure vessel steel, Materials Science and Technology 7 (8) (1991) 686–698.

[13] H. K. D. H. Bhadeshia, MAP_STEEL_DILAT, http://www.msm.cam.ac.uk/map/steel/programs/dilat-b.html.

[14] J. C. Fisher, J. H. Hollomon, D. Turnbull, Kinetics of the Austenite to Martensite Transformation, Metals Transactions 185 (1949) 691–700.

[15] C. Mack, M. S. Bartlett, On clumps formed when convex laminae or bodies are placed at random in two or three dimensions, Mathematical Proceedings of the Cambridge Philosophical Society 52 (1956) 246–250. `doi:10.1017/S0305004100031236`.
URL `http://journals.cambridge.org/article_S0305004100031236`

[16] L. C. Chang, H. K. D. H. Bhadeshia, Austenite films in bainitic microstructures, Materials Science and Technology 11 (9) (1995) 874–882.
URL `http://www.maneyonline.com/doi/abs/10.1179/mst.1995.11.9.874`

[17] W. Rasband, Imagej: Image processing and analysis in java, Astrophysics Source Code Library 1 (2012) 06013.